

Positron-annihilation spectroscopy of native vacancies in as-grown GaAs

C. Corbel and M. Stucky

*Centre d'Etudes Nucléaires de Saclay, Institut National des Sciences et Techniques Nucléaires,
91191 Gif-sur-Yvette Cédex, France*

P. Hautojärvi and K. Saarinen

Laboratory of Physics, Helsinki University of Technology, 02150 Espoo, Finland

P. Moser

Centre d'Etudes Nucléaires de Grenoble, Département de Recherche Fondamentale, 38041 Grenoble Cédex, France

(Received 25 August 1987; revised manuscript received 3 March 1988)

Native vacancy defects are studied in as-grown GaAs materials by positron-lifetime measurements. Direct evidence of native monovacancy-type defects is found in as-grown *n*-type Te-, Sn-, and Si-doped GaAs. However, the same evidence is not found in as-grown semi-insulating In- or Cr-doped GaAs or semi-insulating undoped GaAs or *p*-type GaAs(Zn). It is shown that the positron trapping and annihilation in the native defects are strongly dependent on the position of the Fermi level in as-grown *n*-type GaAs. It is concluded that the configurations of the native monovacancy defects in GaAs (Te or Sn) change with the position of Fermi level. Two Fermi-level-controlled transitions are found: one is located at 0.035 ± 0.015 eV and the other at 0.10 ± 0.02 eV below the conduction band. It is proposed that the two transitions correspond to two charge-state transitions of the arsenic vacancy $V_{As}^{2-} \rightarrow V_{As}^{-}$ and $V_{As}^{-} \rightarrow V_{As}^0$, respectively.

I. INTRODUCTION

Depending on the growth conditions, various localized energy levels are detected in the energy gap of as-grown gallium arsenide by electrical and optical spectroscopy techniques.¹ These levels strongly affect the electronic properties of materials and it is important to determine the atomic structure and the chemical nature of the native defects responsible for them.

However, this identification is still a matter of controversy.^{1,2} A major reason is that the electron paramagnetic resonance (EPR), recognized as the most powerful technique to study the structure of defects in semiconductors, gives signals difficult to analyze in GaAs. The hyperfine structure of the spectra cannot be resolved even with high-resolution techniques. Consequently, controversial models are still proposed for the same energy levels. Intrinsic defects like antisites (As_{Ga}, Ga_{As}), interstitials (As_i, Ga_i), and vacancies (V_{As}, V_{Ga}) as well as residual impurities are considered in these models. For instance,² the midgap electron trap *EL2* found in most GaAs materials has been successively proposed to be V_{Ga}, As_i , a complex involving $V_{Ga} - As_i$, $As_{Ga} - V_{As}$, and recently a pair $As_{Ga} - As_i$.

Therefore, techniques able to directly determine the interstitial or vacancy nature of a defect are expected to yield new and valuable information on the structure of the native defects. Positrons get trapped at vacancy-type lattice defects and consequently, positron annihilation has proved to be a powerful method to study vacancy-type defects on an atomic scale. It has been widely used in metals during the last decade.³⁻⁵ The situation is much different in the field of semiconductors, where only a few studies have shown that positron annihilation can

be successfully applied. Silicon is mostly found to be free of native vacancy defects when it is as-grown and to contain vacancy defects when it is irradiated⁶⁻⁹ or deformed.¹⁰ In contrast to silicon, compound semiconductors like gallium arsenide¹¹⁻¹⁶ or indium phosphide¹⁷ are found to contain native vacancy defects. The concentrations are estimated to be rather high, of the order of $10^{17} - 10^{18}$ cm⁻³. For recent reviews on positron annihilation in semiconductors, see Refs. 18 and 19.

We report in this paper a systematic investigation of the positron annihilation in GaAs materials aiming to characterize native vacancy defects in as-grown crystals. We have measured the positron lifetime and its temperature dependence in Zn-, In-, Cr-, Sn-, Te-, and Si-doped, as well as in undoped, as-grown single crystals. Some preliminary results of this study have been reported earlier.²⁰⁻²³

The positron response in as-grown GaAs depends systematically on the conduction type. In *n*-type GaAs, vacancy-type defects are detected. Their charge is either neutral or negative. The analysis of the results indicates that the native defects are of the monovacancy type. In Te- and Sn-doped GaAs, the defects present three configurations depending on the position of the Fermi level. They become positive in Te- or Sn-doped materials compensated by electron irradiation.

The Fermi-level positions at which the native defects in *n*-type GaAs (Te or Sn) change their configurations suggest that the three distinct configurations are related to the charge states of the arsenic vacancy corresponding to $V_{As}^{2-}, V_{As}^{-}, V_{As}^0$. Two identifications are discussed. (i) The native defects are clean or decorated arsenic vacancies and the three vacancy configurations correspond to $V_{As}^{2-}, V_{As}^{-}, V_{As}^0$. (ii) The native defects are clean or

decorated gallium vacancies and the three vacancy configurations correspond to V_{Ga}^{3-} and to the arsenic-vacancy-arsenic-antisite pair $V_{\text{As}}-\text{As}_{\text{Ga}}, V_{\text{Ga}}^0-\text{As}_{\text{Ga}}$.

In as-grown semi-insulating (si) or *p*-type GaAs, the positron response is consistent with two alternative situations. (i) The native defects are not of the vacancy type. (ii) The native defects are of the vacancy type but with a positive charge, in which case they involve arsenic vacancies.

This paper is organized as follows. The experiments are described in Sec. II and the results are presented in Sec. III. The analysis of the results leads to identify three distinct positron-annihilation states corresponding to the lifetimes 232, 258, and 295 ps, respectively. The 258- and 295-ps annihilation states appear only in *n*-type doped GaAs. The former is reversibly replaced by the latter when temperature increases from 77 to 500 K. Both states disappear after annealing and electron irradiation. The positron trapping model for vacancies in semiconductors, which is used to explain the results, is discussed in Sec. IV. The experimental positron lifetimes found in GaAs are, respectively, attributed to annihilation in bulk (232 ps) and to annihilations in monovacancy defects (258 and 295 ps) in Sec. V. The observation that native defects are detected only in *n*-type GaAs materials is correlated to the charge states of the monovacancy defects in Sec. VI. The properties of the native vacancy defects are analyzed as a function of carrier concentration in Sec. VII. It is concluded in Sec. VIII that the position of the Fermi level determines entirely the positron-annihilation states in as-grown GaAs.

II. EXPERIMENTAL DETAILS

Positron lifetimes were measured in GaAs samples of $5 \times 5 \times 0.2 \text{ mm}^3$ cut from various single crystals (see Table I). The crystals had been grown either by liquid-encapsulated Czochralski (LEC) method or by horizontal Bridgman method (HB). In the text hereafter the following notation for the samples will be used: the sample labeled by *n*-GaAs(Te: 1.5×10^{16}) is *n*-type doped with Te atoms and has a net carrier concentration of $1.5 \times 10^{16} \text{ cm}^{-3}$. Experiments were performed in the as-grown, isochronally annealed and in irradiated states of the samples. Two identical sample pieces from the same wafer were sandwiched with a $10\text{-}\mu\text{Ci}$ positron source prepared by evaporating $^{22}\text{NaCl}$ solution onto a $5\text{-}\mu\text{m}$ Al or $1\text{-}\mu\text{m}$ Ni foil.

The lifetime spectra with 10^6 counts were recorded using two fast-fast coincidence systems with time resolutions of 230 and 300 ps for the full width at half maximum (FWHM). The source corrections, i.e., the contribution of positrons annihilating in the source materials, were estimated by measuring well-characterized defect-free metals and Si samples. Following corrections were used for the GaAs sample: 2.5% of 450 ps and 0.1–0.3% of 800 ps for the Al-foil source and 7.5% of 150 ps and 4.5% of 450 ps for the Ni-foil source.

After source corrections the lifetime spectra were fitted to a sum of exponential decay components

$$n(t) = n_0 \sum_i (I_i / \tau_i) \exp(-t / \tau_i) \quad (1)$$

TABLE I. Characteristics of the measured GaAs single crystals. They are grown by the Bridgman (HB) or Czochralski (CZ) method and provided by Thomson (CFS), Radiotechnique (RTC), Laboratoire d'Electronique, de Technologie et d'Instrumentation (L), Cambridge Instruments (CI), Electronic Materials (MCP), and Boliden (B). The carrier concentrations are measured at 300 K.

Dopant	Growth method	Supplier	Carrier concentration (cm^{-3})	Dislocation density (cm^{-2})	Orientation
Zn	HB	RTC	2.0×10^{18}		$\langle 100 \rangle$
Zn	CZ	CI	5.4×10^{17}	2.0×10^4	$\langle 100 \rangle$
Zn	CZ	CI	6.2×10^{16}	2.2×10^4	$\langle 100 \rangle$
Cr	CZ	RTC	semi-insulating		$\langle 100 \rangle$
undoped	CZ	CFS	semi-insulating		$\langle 100 \rangle$
undoped	CZ	L	semi-insulating		$\langle 100 \rangle$
In	CZ	L	semi-insulating		$\langle 100 \rangle$
Sn	CZ	CI	1.0×10^{16}		
Sn	CZ	CI	1.6×10^{16}		$\langle 111 \rangle$
Sn	CZ	CI	1.2×10^{17}	2.68×10^4	$\langle 100 \rangle$
Te	CZ	CI	1.5×10^{16}	$< 10^4$	$\langle 100 \rangle$
Te	CZ	CI	2.0×10^{17}	2.62×10^4	$\langle 100 \rangle$
Te	HB	MCP	5.0×10^{18}	1.0×10^4	$\langle 100 \rangle$
Si	CZ	B	1.7×10^{18}		$\langle 100 \rangle$
Si	HB	RTC	2.3×10^{18}		$\langle 100 \rangle$

convoluted with the Gaussian resolution function of the spectrometer. Here n_0 is the total number of observed annihilation events and I_i denotes the relative intensity of the component having the lifetime τ_i . Only one or two components were resolved in our experimental spectra. From the lifetime and intensity values we calculated also the average lifetime

$$\tau = I_1\tau_1 + I_2\tau_2 \quad (2)$$

which is insensitive to the uncertainties in the decomposition procedure. The fitting was performed so that the variance was at minimum and that the average lifetime τ coincided with the center of mass of a spectrum within ± 1 ps.

The average lifetimes measured from the same samples with different lifetime spectrometers and different positron sources coincided typically within 2 ps. On the other hand, the decompositions were found to be sensitive to the time resolution. Especially, when the ratio of τ_2/τ_1 decreased below 1.5, the higher resolution of 230 ps (FWHM) was found to be crucial to get reliable decompositions.

The isochronal annealings were performed under vacuum (30 min, 10^{-6} torr) between 300 and 850 K. After each annealing, the positron-lifetime spectra were measured at 300 K. After annealings above 750 K, the lifetimes were measured also at 100 K.

Lightly Te- and Sn-doped GaAs samples were irradiated at room temperature with 1.5-MeV electrons to make them semi-insulating. Irradiations were performed with the Van der Graaf accelerator of the Ecole Normale in Paris. The lifetimes were measured at 100 and 300 K in the as-irradiated state.

Electrical measurements (capacitance-voltage) and deep-level transient spectroscopy (DLTS) measurements have also been performed in GaAs(Sn: 1.6×10^{16}) to check the quality of the samples. The measurements indicated the presence of five localized levels in the gap. The levels acted as electron traps. Their total concentration was less than 10^{16} cm^{-3} . Hall measurements were also performed at 300 and 77 K for several samples to check the carrier concentrations given by the suppliers.

III. EXPERIMENTAL RESULTS

In this section, we examine successively, how in GaAs the positron-lifetime spectra depend on the doping, temperature, annealing, and irradiation treatment of the samples.

A. Lifetime spectra at 100 and 300 K: doping effect

The decomposition of the lifetime spectra measured at low temperature is often difficult and rather ambiguous even at the higher resolution of 230 ps (FWHM). Reasons for this will be discussed in Secs. III B and VII A. Therefore we present in Table II only the *positron average lifetimes* measured at 100 K for the as-grown states.

Four trends appear clearly in the *positron average lifetimes* τ given in Table II at 100 K for the as-grown sam-

TABLE II. Positron lifetimes at 100 K in as-grown GaAs. The effect of the carrier nature and concentration. The carrier concentrations are measured at 300 K.

Dopant	Type	Carrier concentration (cm^{-3})	τ (ps)
Zn	<i>p</i>	2.3×10^{18}	230 ± 1
Zn	<i>p</i>	5.0×10^{17}	235 ± 1
Zn	<i>p</i>	6.0×10^{16}	234 ± 1
Cr	si		232 ± 1
undoped	si		234 ± 1
Sn	<i>n</i>	1.0×10^{16}	256 ± 1
Sn	<i>n</i>	1.2×10^{17}	246 ± 1
Te	<i>n</i>	1.5×10^{16}	245 ± 1
Te	<i>n</i>	2.0×10^{17}	246 ± 1
Te	<i>n</i>	5.0×10^{18}	245 ± 1
Si	<i>n</i>	2.3×10^{18}	236 ± 1

ples. (i) The average lifetime τ remains practically constant in *p*-type GaAs when the doping concentration varies. (ii) In semi-insulating GaAs, the average lifetime τ is the same in doped or undoped GaAs and its value of 234 ± 2 ps is quite close to that found in *p*-type GaAs. (iii) The average lifetime τ is systematically higher in *n*-type GaAs than in si or *p*-type GaAs. (iv) The average lifetime τ is sensitive to the doping concentration in *n*-type GaAs and ranges from 240 to 260 ps.

These four trends remain valid for the average lifetime measured at 300 K (Table III). In addition, the *decompositions of the lifetime spectra* also shown in Table III depend on the doping. Only a single lifetime is resolved in *p*-type and si GaAs, but one or two components are resolved in *n*-type GaAs depending on the carrier concentration. Two lifetimes are easily resolved in the three lightly doped *n*-GaAs (Te: 1.5×10^{16}), *n*-GaAs (Sn: 1.0×10^{16}), and *n*-GaAs (Sn: 1.6×10^{16}) specimens. The longer component τ_2 is the same in the three samples and has a value of 295 ± 5 ps.

In *n*-GaAs (Te: 2×10^{17}) and *n*-GaAs (Sn: 1.2×10^{17}) the resolution of the lifetime spectra into two components is more difficult. The longer lifetime appears with a value of 265 ps, which is lower than in the lightly *n*-type doped samples.

In the heavily-doped *n*-GaAs (Te, Se: $> 10^{18}$) samples the free decompositions are possible only with the lifetime spectra measured with the higher (230 ps FWHM) time resolution. The long lifetime is then 258 ± 4 ps and thus definitely lower than that of 295 ps found in the lightly *n*-type doped samples.

B. Temperature effects on the lifetime spectra

The comparison of the measurements performed at 100 and 300 K shows that the variations of the lifetime spectra with the temperature depend on the doping of the samples. This phenomenon is clearly illustrated in Figs. 1–3 showing the variation of the average lifetime τ in *p*-, si, and *n*-type GaAs in the range 100–400 K. Let us mention that all the curves in Figs. 1–3 are reproducible

TABLE III. Positron-lifetime spectra at 300 K in as-grown GaAs. The effect of the carrier nature and concentration at 300 K.

Dopant	Type	Carrier concentration (cm ⁻³)	τ (ps)	τ_1 (ps)	τ_2 (ps)	I_2 (%)
Zn	<i>p</i>	2.3×10^{18}	229±1			
Zn	<i>p</i>	5.0×10^{17}	232±1			
Zn	<i>p</i>	6.0×10^{16}	232±1			
Cr		si	235±1			
undoped		si	232±1			
undoped		si	231±1			
In		si	233±1			
Sn	<i>n</i>	1.0×10^{16}	261±1	141± 7	291± 3	80±2
Sn	<i>n</i>	1.6×10^{16}	264±1	155± 7	297± 2	77±2
Sn	<i>n</i>	1.2×10^{17}	239±1	167±11	266± 4	73±5
Te	<i>n</i>	1.5×10^{16}	247±1	156± 7	284± 3	71±2
Te	<i>n</i>	2.0×10^{17}	242±1	184±10	265±10	71±7
Te	<i>n</i>	5.0×10^{18}	238±1	193±35	254±12	74±30
Si	<i>n</i>	1.7×10^{18}	238±1	174±14	258± 4	76±8
Si	<i>n</i>	2.3×10^{18}	248±1	125±15	262± 2	90±2

and reversible.

No temperature effect is found in *p*-type GaAs(Zn) and in doped or undoped si GaAs samples (Fig. 1). A strong effect occurs in lightly doped *n*-GaAs(Te: 1.5×10^{16} and Sn: 1.0×10^{16}) where τ goes through a maximum at about 200 K. The maximum is still seen but much reduced in *n*-GaAs(Sn: 1.2×10^{17} and Te: 2×10^{17}) (Fig. 2). The maximum seems to disappear in heavily doped *n*-type GaAs (Fig. 3). The nature of the donors seems to influence the curves $\tau(T)$. An increase of 10 ps of the positron lifetime is observed in *n*-GaAs(Si: 2.3×10^{18}), whereas a slight decrease of 5 ps is observed in heavily doped *n*-GaAs(Te: 5.0×10^{18}).

The decompositions of the lifetime spectra in *n*-

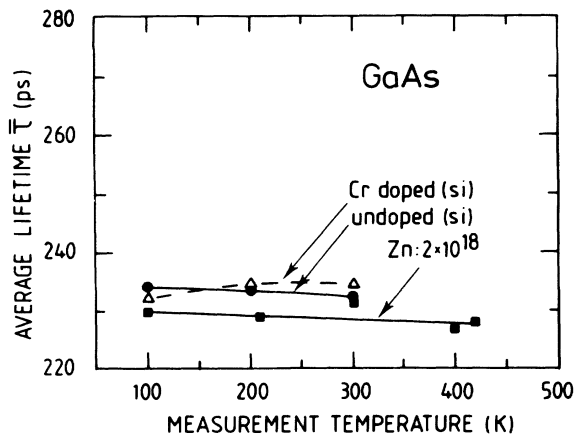


FIG. 1. Average positron lifetime as a function of temperature in as-grown *p*-type GaAs(Zn), semi-insulating undoped GaAs and doped GaAs(Cr).

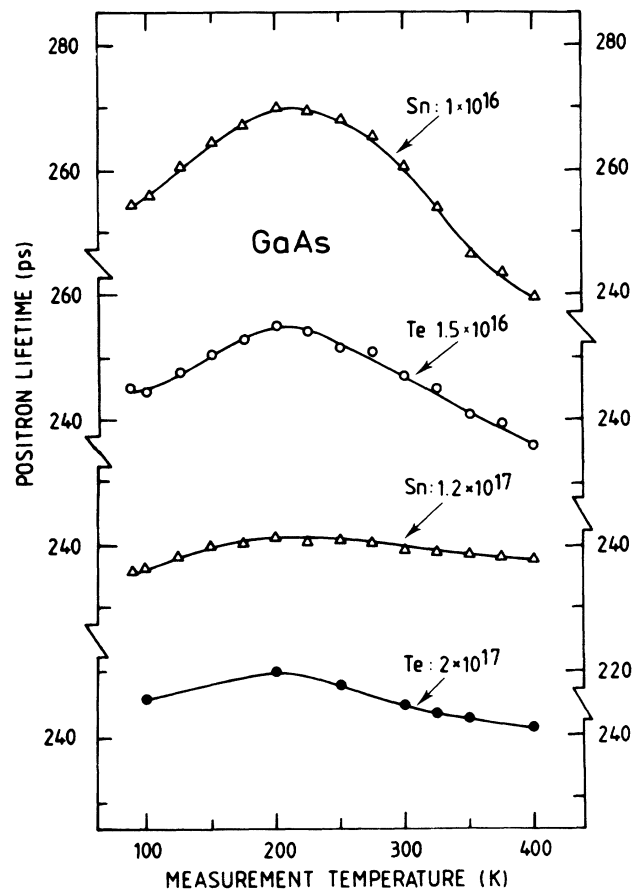


FIG. 2. Average positron lifetime as a function of temperature in as-grown *n*-doped GaAs(Sn: 1.0×10^{16}), GaAs(Te: 1.5×10^{16}), GaAs(Sn: 1.2×10^{17}), and GaAs(Te: 2.0×10^{17}). The carrier concentrations at 300 K are given in cm⁻³.

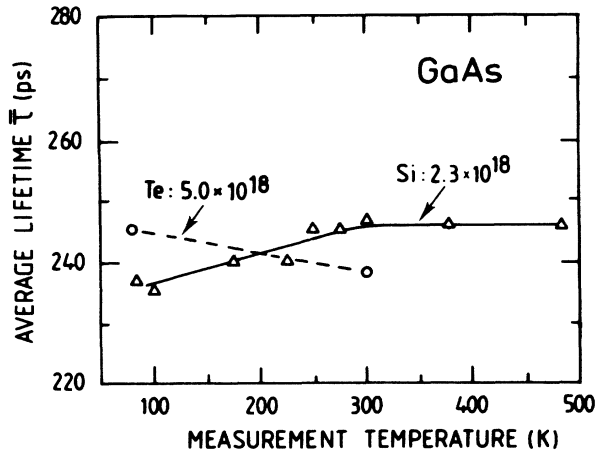


FIG. 3. Average positron lifetime as a function of temperature in as-grown heavily n -doped GaAs(Te: 5.0×10^{18}) and GaAs(Si: 2.3×10^{18}).

GaAs(Te: 1.5×10^{16}) and n -GaAs(Sn: 1.0×10^{16}) as a function of temperature are shown in Figs. 4 and 5, respectively. Most striking is the behavior of τ_2 . At low temperatures it reaches a value of 260 ps and above 100 K it starts to increase with temperature towards a level of 290 ps. Above 300 K τ_2 stays constant, but the intensity I_2 decreases strongly.

From Figs. 4 and 5 one can see why the decomposition is difficult at low temperatures: the values of τ_1 and τ_2 are close to each other. Also at high temperatures ($T > 300$ K) the decomposition becomes more uncertain, because I_2 decreases below 50%.

Figure 6 shows the decompositions in n -GaAs(Sn: 1.2×10^{17}) as a function of temperature. The lifetime τ_2 is about 260 ps at low temperatures and stays at this level up to 250 K. Above this temperature it starts to increase slowly towards 290 ps. So again, as at lower doping level, τ_2 increases with temperature. However, the increase of τ_2 is shifted to higher temperatures and occurs also on a wider temperature range. The error bars in Fig. 6 are rather large due to the low values of the average lifetime τ and small intensities I_2 especially above 400 K.

C. Annealing of the as-grown samples

Annealing effects on the positron-lifetime spectra have been studied in n -type GaAs (Te or Sn). They are found to depend only weakly on the carrier concentration (Fig. 7) and to be independent of the nature of the donor (Fig. 8). As seen in Figs. 7 and 8, the average lifetime decreases in the temperature range 680–850 K. In the lightly doped samples, the annealing stage of the average lifetime corresponds to a decrease of the intensity I_2 of the 295-ps component. The decomposition of the lifetime spectra remains unchanged up to 650 K. Two components are still resolved in the positron-lifetime spectra after annealing at 700 K, but above this temperature, the intensity I_2 decreases. After annealing above 850 K, only one single lifetime is resolved. This lifetime 232 ± 3 ps is

the same as the one measured in as-grown, p -type or n -type GaAs. We have checked that the specimens were still n -type at 300 K after annealings at 850 and 1000 K.

D. Compensation by irradiation

The results after 300-K irradiation at a dose sufficient to compensate GaAs(Te: 1.5×10^{15}) and GaAs(Sn: 1.6×10^{16}) specimens are given in Table IV. The average positron lifetime measured at 100 or 300 K is lower than its initial value and reaches a value, of 230–240 ps, slightly higher than in p -type or n -type GaAs. The decomposition of the lifetime spectra into two components at 300 K is difficult, even if the 295 or 258 ps lifetime are fixed. More results on the irradiation effects can be found in Refs. 20–24.

E. Positron annihilation states

In GaAs, the lifetime spectra consist of one or two components and the average lifetimes vary in the range 230–270 ps. This means that the electron-positron pairs

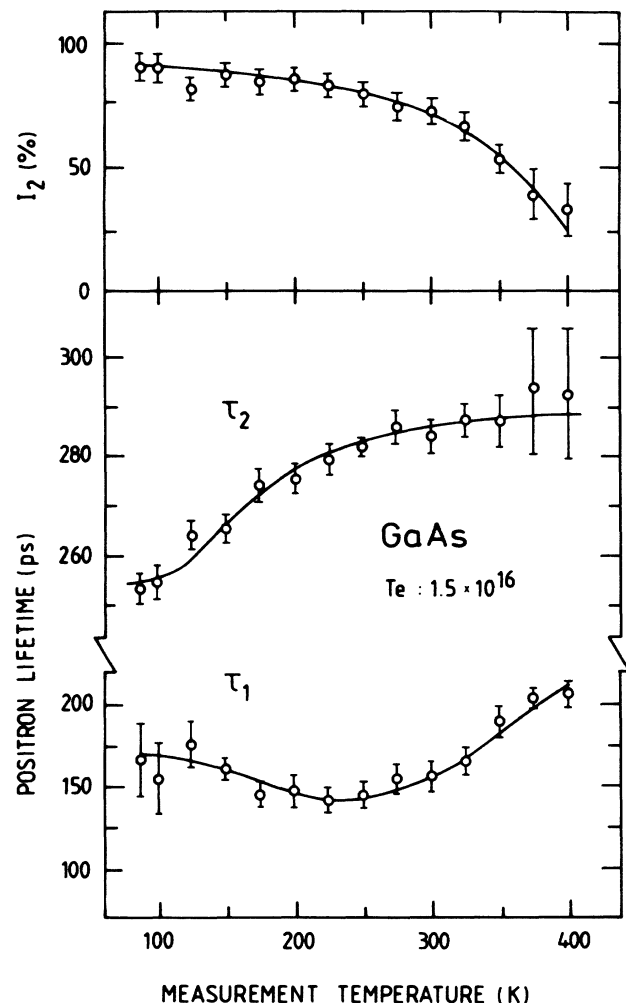


FIG. 4. Decomposition of the positron-lifetime spectra as a function of temperature in as-grown lightly n -doped GaAs(Te: 1.5×10^{16}).

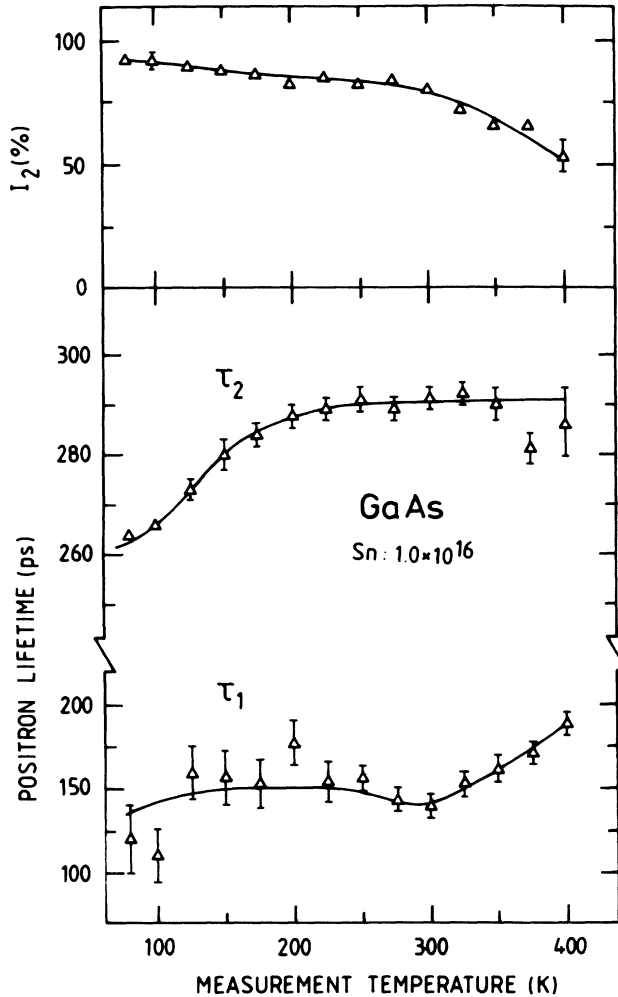


FIG. 5. Decomposition of the positron-lifetime spectra as a function of temperature in as-grown lightly n -doped GaAs (Sn: 1.0×10^{16}).

can annihilate from different states in GaAs. Let us see the number of these states and their associated lifetimes.

In several samples, a decay constant of 232 ± 3 ps has been found, which remains constant in the temperature range 100–400 K. These characteristics suggest strongly that the 232-ps decay constant corresponds to a well-defined positron state in GaAs that we will call in the following the 232-ps annihilation state.

A second annihilation state gives rise to the lifetime of 295 ps which is reproducibly observed in several lightly n -type doped samples at 300 K and between 250–400 K. The 295-ps annihilation state occurs in the Te- and Sn-doped specimens when the carrier concentration is about 10^{16} cm^{-3} . It is always observed in competition with another annihilation state.

Clearly at least a third annihilation state takes place in the n -type GaAs, since the decompositions in Figs. 4–6 change with temperature. The lifetime τ_2 in the n -type doped (10^{16} – 10^{17} cm^{-3}) samples reaches a value of 260 ± 5 ps at lower temperatures. In addition, at room temperature the free decompositions of the heavily n -type

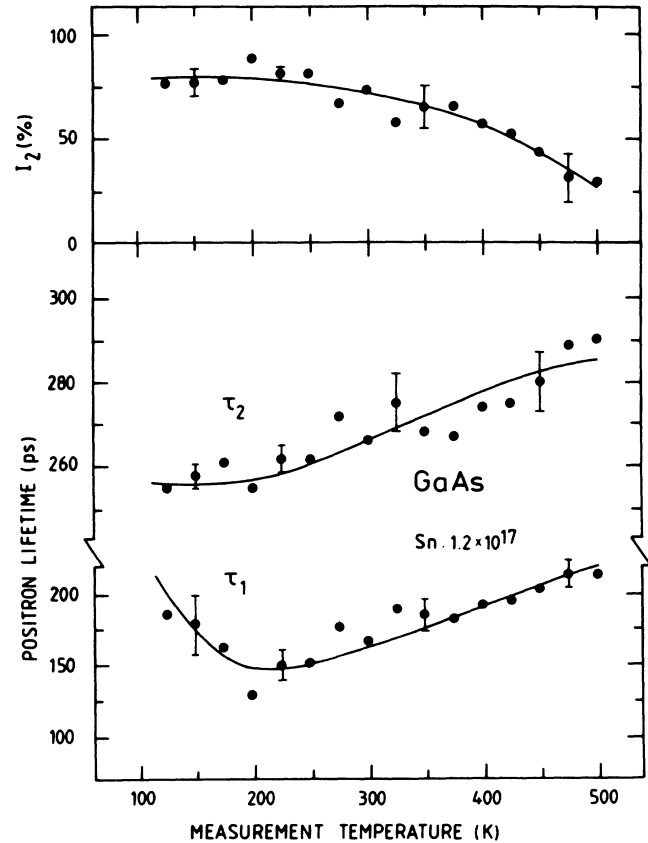


FIG. 6. Decomposition of the positron-lifetime spectra as a function of temperature in GaAs (Sn: 1.2×10^{17}). Below 125 K the decomposition of the spectra is not possible.

doped ($> 10^{18} \text{ cm}^{-3}$) materials give a second lifetime of 258 ± 3 ps and below room temperature any spectra measured from these samples can be fitted by fixing τ_2 to 258 ps. Also the lifetimes measured after electron irradiations^{20–24} are close to 260 ps. These facts lead us to assume that a lifetime of 258 ± 3 ps corresponds to a well-

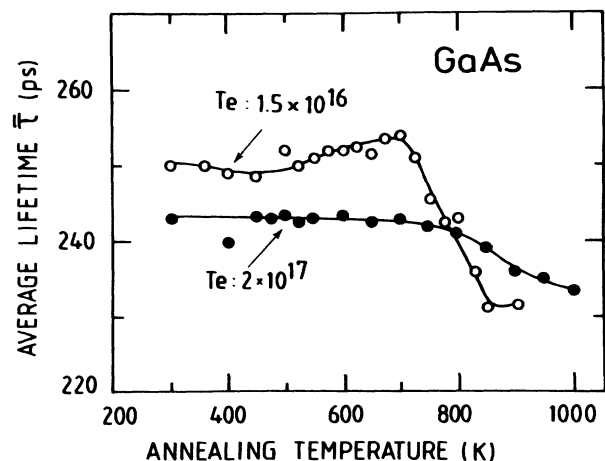


FIG. 7. Average positron lifetime as a function of annealing temperature in as-grown n -type doped GaAs (Te). The influence of the donor concentration in GaAs (Te).

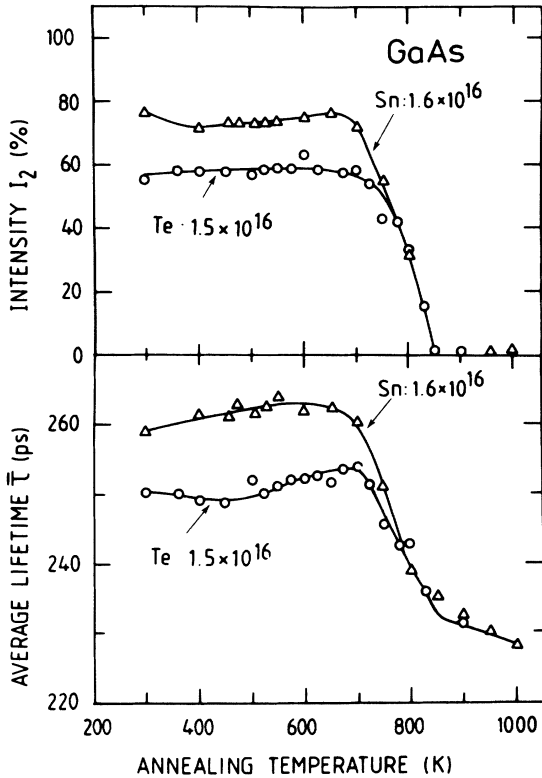


FIG. 8. Average positron lifetime and the intensity of the 295-ps component as a function of annealing temperature in as-grown *n*-type doped GaAs (Te or Sn). The influence of the nature of the dopant in lightly doped GaAs ($n \approx 10^{16} \text{ cm}^{-3}$).

defined positron-annihilation state. Any value of τ_2 between 258 and 295 ps in Figs. 4–6 and Table III can be interpreted as a superposition of these two annihilation states, as will be discussed later.

F. Summary of experimental findings

In summary, *three annihilation states* have been identified in as-grown GaAs corresponding to the lifetimes of 232, 258, and 295 ps. Their existence depends on the doping type of the samples and furthermore, on the carrier concentration in *n*-type materials.

The 232-ps annihilation state occurs in *p*-type GaAs for any level of the doping. It also occurs in semi-insulating samples doped or undoped. It is the single annihilation

TABLE IV. Average positron lifetime τ in ps before and after compensation by 1.5-MeV electron irradiation at 300 K. The measurement temperature is also given. The conduction type of the samples is indicated in parentheses.

Sample	As-grown (300 K)	Irradiated (300 K)	($10^{17} \text{ e}^- \text{ cm}^{-2}$) (100 K)
Te: 1.5×10^{16}	250±1 (<i>n</i>)	233±1 (<i>si</i>)	232±1 (<i>si</i>)
Sn: 1.6×10^{16}	264±1 (<i>n</i>)	241±1 (<i>si</i>)	

state occurring in these materials. In *n*-type GaAs it is also gradually reached at temperatures above 300 K and it is found at any temperatures after annealing above 800 K.

The 258-ps annihilation state is observed in the range 100–400 K in highly *n*-type doped GaAs (Te or Si: 10^{18}) materials. The 258-ps annihilation state is observed below 200 K in GaAs (Te or Sn: 10^{17}) and below 100 K in GaAs (Te or Sn: 10^{16}). It disappears progressively above 200 K and is replaced completely or partially by the 295-ps annihilation state. The 295-ps annihilation state is replaced by the 232-ps annihilation state as the temperature increases, and has nearly disappeared at 400 K.

The 232-ps annihilation state and the 295-ps annihilation state have been previously observed in undoped GaAs at room temperature by Kerr *et al.*,¹² Dannefaer *et al.*,^{13,14} and Dlubek *et al.*¹⁶ Lifetimes of about 260 ps have been reported in as-grown¹⁵ as well as in electron irradiated samples.^{22–24} In addition, the measurements by Dlubek *et al.*¹⁶ at 300 K exhibited the same systematic trends as ours. The average positron lifetime was always higher in *n*-type GaAs than in *p*-type GaAs. Their average positron lifetime in *p*-type and *si* GaAs was 230 ± 3 ps as in our single crystal samples and only one positron lifetime was resolved. The average lifetime varied in *n*-type doped specimens depending on the doping level. The decomposition of the lifetime spectra varied also with the doping level. Dannefaer and Kerr¹⁵ have also noticed that the 295-ps annihilation state exists only in lightly doped *n*-type GaAs, whereas in heavily doped GaAs (Si: 10^{18}) they found a second lifetime with the value 260 ps. The change of τ_2 from 260 to 295 ps as a function of temperature has recently been found also in several undoped lightly *n*-type GaAs.²⁵

In the following, we will focus on these systematic trends, not emphasized previously, and on the temperature dependence of the lifetime spectra. We will show that a coherent picture of the positron response emerges, when the annihilation characteristics are correlated to the position of the Fermi level.

IV. POSITRON TRAPPING IN GaAs

In Sec. III, we have associated the lifetimes of 232, 258, and 295 ps measured in GaAs to three distinct annihilation states. These lifetimes are due to annihilations arising from different positron states. Annihilation from positronium states would lead to much longer lifetimes, of about 1000 ps, and consequently can be excluded. We explain the existence of the 258- and 295-ps lifetimes by the trapping of positrons in native vacancy defects. The trapping model is well established in metals and can be extended to semiconductors. However, in semiconductors, a new parameter, which is the charge of the vacancy defects, has to be considered. The results presented in Sec. III will therefore be discussed as follows.

In this section, we shall recall the main features of the positron trapping model and discuss the effects of the charge state of vacancy defects on positron lifetime and positron trapping. We shall see that the positive charge of positrons prevents the trapping by positive vacancy de-

fects. In semiconductors, positron trapping is limited to vacancy defects which are neutral or negatively charged.

In Sec. V, we shall assign the 232-ps lifetime to annihilation in the bulk. We shall assign the 295-ps lifetime to annihilation in a position trap denoted by P1 and 258-ps lifetime to a positron trap P2. We shall show that P1 and P2 are monovacancy-type defects.

The results show that the 232-ps state occurs in *p*-type Si, and *n*-type GaAs and that the 295- and 258-ps states occur only in *n*-type GaAs. We shall draw the implications of this property in Sec. VI. We shall arrive at the conclusion that the P1 and P2 defects can involve either the gallium vacancy or the arsenic vacancy since, according to several theoretical and experimental works, both are neutral or negative in the *n*-type GaAs.

In Sec. VII, we shall correlate the evolution of the positron-lifetime spectra in *n*-type GaAs to the position of the Fermi level. We shall be led to propose that the positron traps P1 and P2 correspond to two configurations of a same native vacancy defect. The transition P2→P1 (i.e., the positron-lifetime change 258→295 ps) occurs when the Fermi level moves down in the gap to $E_C - 0.035$ eV (E_C is the energy of the bottom of the conduction band). Also the transition P1→bulk, i.e., the lifetime change 295→232 ps, seems to be Fermi-level controlled and occurs when the Fermi level moves down to $E_C - 0.10$ eV. We shall propose that these two transitions reflect the charge-state transitions of the arsenic vacancy $V_{As}^{2-} \rightarrow V_{As}^-$ and $V_{As}^- \rightarrow V_{As}^0$, respectively.

A. Positron trapping model

Positrons being positively charged are able to get trapped in vacancy defects where positron-ion repulsion is locally reduced. Annihilations at vacancy defects give characteristics clearly different from those arising from annihilations in the bulk. The positron lifetime is longer when the annihilation occurs in a vacancy defect than in the bulk, because the electron density is lower in a vacancy defect. Positron trapping is well identified in metals. For example, in iron the positron has a lifetime of 110 ps when delocalized in the bulk,²⁶ of 142 or 165 ps when localized in dislocations,²⁷ and of 170 ps when localized in a monovacancy.²⁶

A quantitative analysis of the positron-lifetime spectra can be done using the positron trapping model.²⁸ In this model, the total trapping rate κ for a concentration c_d of defects is given by

$$\kappa = \mu_d c_d, \quad (3)$$

where μ_d denotes the specific trapping rate per defect. The annihilation in the vacancy-type defect is characterized by a lifetime τ_d longer than the lifetime τ_b in the bulk. If a trapped positron does not escape from the defect, a two-component exponential lifetime spectrum

$$n(t)/n_0 = (I_1/\tau_1)\exp(-t/\tau_1) + (I_2/\tau_2)\exp(-t/\tau_2) \quad (4)$$

with

$$1/\tau_1 = 1/\tau_b + \kappa, \quad (5)$$

$$\tau_2 = \tau_d, \quad (6)$$

follows from the trapping model for one type of defect. The validity of the model can be tested from Eq. (4) or from the following relationship:

$$1/\tau_0 = I_1/\tau_1 + I_2/\tau_2 = 1/\tau_b. \quad (7)$$

The total trapping rate can be obtained for the following relations:

$$\kappa = \frac{I_2}{I_1} \left[\frac{1}{\tau_b} - \frac{1}{\tau_2} \right] = \frac{1}{\tau_b} \frac{\tau - \tau_b}{\tau_2 - \tau}, \quad (8)$$

where $\tau = I_1\tau_1 + I_2\tau_2$ is the average lifetime.

If the specific trapping rate is known, one can calculate the concentration of the vacancy-type defects corresponding to the lifetime τ_2 . For vacancies in metals, μ varies in the range 10^{-9} – 10^{-8} cm³s⁻¹.³ This means that in metals with a typical specific trapping rate of 10^{-8} cm⁻³ vacancies are detected by positrons for concentrations above 10^{15} cm⁻³.

When there is more than one type of defect and when the experimental lifetime spectra can be resolved only in two components, usually the shorter defect lifetimes are mixed into τ_1 and the longest one comes out as τ_2 . In this case Eqs. (5) and (7) are not fulfilled and the trapping rate from Eq. (8) gives a lower bound of the defect concentration.

B. Positron trapping and charge state of vacancy defects

The above trapping model can be applied to semiconductors. However, a new factor, the charge of a vacancy defect, has to be considered. In semiconductors, vacancy defects can have several charge states. To what extent shall the characteristics of positron trapping in a vacancy defect be sensitive to its charge state? Let us focus on the specific trapping rate and the positron lifetime, which are the interesting characteristics in this paper.

The first question concerns the ability of positively charged vacancy defects to trap positrons. It can be expected that no trapping occurs in positively charged vacancy defects, since positrons are positive. It is effectively what we have observed after irradiation in GaAs for the As vacancy.^{22–24} We consider that this result can be expected to other vacancy defects in GaAs and other semiconductors.

The second question to be considered is the value of the specific trapping rate. Very few data are available. From neutron irradiation experiments in silicon Dannefaer *et al.*⁷ have estimated that the trapping rate in divacancies is 4×10^{-9} cm⁻³s⁻¹, in good agreement with the value of 5×10^{-9} cm⁻³s⁻¹ deduced from electron irradiation experiments of Shimotomai *et al.*⁹ From electron irradiation in GaAs,²² we can estimate that the specific trapping rate per arsenic vacancies, V_{As}^{2-} , is about 6×10^{-9} cm⁻³s⁻¹. These values are comparable to the values of the specific trapping rates for monovacancies in metals, which typically are of the order of 10^{-8} s⁻¹.^{3–5} However, clear theoretical or experimental information is still missing on the following points: (i) the variation of the specific trapping rate with the charge state of a vacancy defect, (ii) the temperature dependence of trapping

for a given charge state, and (iii) the trapping mechanism and its dependence on the position of the defect level in the gap. Some comments can be made. About (i), an increase of the trapping rate is expected when the charge state becomes more negative. About (iii), by comparison with trapping of holes, Dannefaer *et al.*⁸ have suggested that multiphonon trapping process may occur, but there is no experimental evidence for such a process in GaAs.

The third question arises about the variation of the lifetime of a trapped positron when the charge state of the vacancy changes. The positron lifetime in a vacancy depends on the electronic density seen by the trapped positron. Puska's calculations²⁹ have shown that the additional or removal of an extra electron in an ideal vacancy has only a small effect of the order of 1–3 ps. This is comparable to the effect of the decoration of a vacancy by a substitutional impurity in metals.³⁰ The positron density distribution follows the electron charge transfer with nearly no effect on the overlap of the electron and positron wave functions. However, in semiconductors the configuration of a vacancy can be strongly perturbed when the vacancy changes its charge state. The local rearrangement of the lattice in the vicinity of the vacancy may result into relaxation or even distortion (Jahn-Teller effect) when the defect level is degenerated. Calculations in metals have shown that the positron lifetime is extremely sensitive to the configuration of a vacancy defect. For example, in Au an inwards relaxation of the first neighbors of the vacancy by 5% is sufficient to reduce the lifetime by 20%, from 200 to 166 ps.³⁰ Recent calculations on semiconductors reproduce the same effect: an outwards relaxation by 5% increases the positron lifetime trapped in a Si vacancy by 30 ps.³¹ On the basis of these calculations, one therefore expects that in semiconductors, the various charge states of a vacancy defect correspond to positron lifetimes, which can be experimentally distinguished ($\Delta\tau > 10$ ps).

At last, there is the question of the positron trapping by negatively charged ions which may occur at low temperature. Such trapping leads to lifetimes comparable to the bulk and so can be distinguished from trapping in vacancy-type defects. If both types of trapping exist simultaneously, complications may arise in the decomposition of the lifetime spectra. See discussion in Sec. VII A 1.

V. POSITRON ANNIHILATION STATES IN GaAs

In this section, we present the elements which lead us to attribute the 232-ps lifetime to annihilation in bulk and the 295 and 258 ps to annihilation in native monovacancies, which may be isolated or probably associated to other types of point defects.

A. Bulk annihilation in GaAs

The properties which lead us to assign the value of 232 ps to positron annihilation in bulk are the following. First, the value of 232 ± 3 ps is the minimum single positron lifetime we have measured in GaAs. Second, it is

found in as-grown and *p*-type doped GaAs and after annealing above 850 K in *n*-type GaAs. Third, the lifetime of 232 ps in *p*-type and si GaAs is insensitive to the temperature in the range 77–400 K. Fourth, all the decompositions of the positron-lifetime spectra measured above 280 K (Table III, Figs. 4–6) are consistent with the one-defect trapping model, in which the positron has a bulk lifetime of 232 ps as calculated from Eq. (7). The decompositions below 250 K in Figs. 4–6 are more complicated because some additional shallow traps are also active (see Sec. VI A).

The assignment of 232-ps lifetime to the bulk in GaAs is in good agreement with the values previously proposed by Dannefaer *et al.*¹³ and Dlubek *et al.*¹⁶ The lifetime of 232 ps is quite close to the lifetime of 230 ± 3 ps we measured for the bulk in Ge²¹ and longer than the lifetime of 220 ps we measured in Si. We find nearly the same bulk lifetime in Ge and GaAs, which is expected, since the nearest-neighbor distance is the same in both crystals and the atomic numbers are $Z_{\text{Ga}} = 31$, $Z_{\text{Ge}} = 32$, and $Z_{\text{As}} = 33$ resulting in the same average valence electron density.

A bulk lifetime of about 220 ps has also been proposed in GaAs by Dannefaer *et al.*¹⁴ This is based on an indirect argument. In si GaAs and Zn-doped GaAs, the authors are able to resolve a long positron lifetime of about 265 ps, although the average lifetime is also 230 ps, which is practically the same as we observed. To our experience, at this level of the average lifetime the spectra in GaAs are of single component. A lifetime of 220 ps seems to us to be too low for GaAs on the basis of the lifetimes found in Si (220 ps) and Ge (230 ps). Calculations of the bulk lifetimes in semiconductors performed by Puska *et al.*^{29,31} yield to the same conclusion for the following reasons: the GaAs lattice is more open than the Si one and thus has smaller valence electron density in the interstitial regions where a positron is confined. The energy gap of the GaAs is not much different from that of Si and thus the polarizability of valence electrons (enhancement effect) is about the same in both lattices. Theoretical calculations with the same over all enhancement factor for Si, GaAs, and all other III-V compounds give good agreement with experiments including $\tau_b = 232$ ps (but not 220 ps) for GaAs.^{29,31}

B. Positron traps P1 and P2 in GaAs

The second lifetimes of 258 and 295 ps are 10% and 30% longer than the bulk lifetime of 232 ps. Such long lifetimes can occur from the annihilation of positrons localized in vacancy defects.

The lifetime of 295 ps is the longest lifetime found in as-grown GaAs. It appears in spectra which are resolved in two components. It corresponds to a positron trap we call P1. The ratio between this lifetime and the bulk one (295 ps)/(232 ps) is 1.26. This value is comparable to the ratio of 1.26 we found in electron irradiated Ge between the lifetime of 290 ps due to monovacancies and the bulk lifetime 230 ps.²¹ This value is close to the ratio of (270 ps)/(220 ps) = 1.22 found in Si between the monovacancy and bulk lifetimes.⁶ All these elements lead us to conclude that the 295-ps lifetime is due to annihilation in a

monovacancy.

The lifetime of 258 ps is found in heavily doped *n*-type GaAs at 300 K (Table III) and in medium and lightly doped *n*-type GaAs at lower temperatures (Figs. 4–6). It is close to the values of 258 ± 3 ps that we found after electron irradiation at high doses.^{19,22} We also attribute the positron lifetime of 258 ps to annihilation in a single vacancy. The ratio of the 258 lifetime to the bulk lifetime, $(258 \text{ ps})/(232 \text{ ps})$, is about 1.10. This ratio is lower than the ratio expected for trapping in monovacancies in metals from the calculations of Puska and Nieminen.³² However, it is in good agreement with those expected in semiconductors from the similar calculations.^{29,31}

Dannefaer and Kerr¹⁵ have recently attributed the 295-ps lifetime to divacancies ($V_{\text{As}}V_{\text{Ga}}$) and the 260 ps one to monovacancies. We have two comments against the divacancy interpretation. First, the recent theoretical estimate for the divacancy is 320 ps.³¹ Second, the 295-ps lifetime transforms to the 258-ps lifetime (Figs. 4–6) which suggests that they originate from a same defect, as will be discussed in Sec. VII.

C. Nature of the native vacancies

In GaAs, two types of clean vacancies exist due to the existence of the Ga and As sublattices: the gallium vacancy $V_{\text{Ga}} - \text{As}_4$ and the arsenic vacancy $V_{\text{As}} - \text{Ga}_4$. Can we relate the positron traps P1 and P2 to these two vacancies?

The lifetime of 295 ps in P1 can be compared to the lifetime of 279 ps calculated by Puska *et al.*²⁹ in an ideal single arsenic vacancy and the lifetime of 258 ps in P2 to the lifetime of 267 ps calculated in an ideal gallium vacancy. However, too little is known about the charge state and relaxation of the vacancies in GaAs to identify, on the basis of these calculations, the positron trap P1 to an arsenic vacancy and P2 to the gallium vacancy. Furthermore, the lifetimes in vacancies in metals are rather insensitive to the decoration, i.e., the substitution of first neighbor atoms by impurities. We can expect the same in semiconductors as far as the charge state is not changed by the decoration. So, the positron traps P1 and P2 are arsenic or gallium vacancies, either free or bound to substitutional defects like impurities or antisites.

Positron trapping in semiconductors is limited to vacancy defects with neutral or negative charges. We can take advantage of this property to guide our identification of the positron traps in GaAs. The charge states of the gallium and arsenic vacancies are still under discussion.^{29,33–37} However, among the controversial models, some seem to agree well with the positron behavior we observed in as-grown and electron irradiated GaAs.^{20–24} These theoretical^{29,33,36} and experimental works^{36,37} propose the following charge states for V_{As} and V_{Ga} . V_{As} has a charge state different in *n*-type GaAs than in si GaAs and *p*-type GaAs; its charge state is positive in si GaAs and *p*-type GaAs. V_{Ga} has the same charge state in *n*-type GaAs and in si GaAs; it is negative or neutral. These properties of the charge states of V_{As} and V_{Ga} will sustain the identification that we shall propose in Secs. VI and VII for P1 and P2. Our identifi-

cation does not support the calculations of Baraff and Schlüter,^{34,35} according to which V_{As} is positive in any type of GaAs.

VI. POSITRON ANNIHILATION STATES IN GaAs AND CONDUCTION TYPE

It has been shown in Sec. III that positrons behave similarly as a function of the temperature in *p*-type and si as-grown materials, but exhibit a completely different behavior in *n*-type specimens. In this section, the positron behavior is separately discussed in *p*-type GaAs, si GaAs, and then *n*-type GaAs.

As previously noted (Sec. III), the measurements of Dlubek *et al.*¹⁶ at 300 K exhibit the same systematic trends as ours. The average positron lifetime at 300 K is always higher in *n*-type GaAs than in si or *p*-type GaAs. The average positron lifetime in *p*-type and si GaAs is 230 ± 2 ps as in our single crystal samples and only one positron lifetime is resolved. The free decomposition of the lifetime spectra into two components is easy in lightly *n*-type GaAs samples and a lifetime of 295 ps appears in the spectra. In heavily *n*-type GaAs, when the carrier concentration is of the order of 10^{18} cm^{-3} , the lifetime τ_2 decreases to 258 ps making the decomposition of the lifetime spectra more difficult. We shall focus on these systematic trends in Sec. VII after having discussed here the doping effects on positron lifetime.

A. Bulk annihilation in *p*-type GaAs(Zn)

The lifetime is 232 ps regardless of the temperature or the carrier concentration in *p*-type GaAs(Zn). This means that there are no positron traps in *p*-type GaAs(Zn), since we observe only the 232-ps bulk annihilation; therefore no neutral or negative vacancy defects are present in the samples. We conclude that the *p*-type GaAs(Zn) samples either contain no vacancy defects or contain positively charged vacancy defects.

The presence of gallium vacancies in these samples seems to be excluded since they are negative or neutral in *p*-type materials (possibly positive in highly doped materials). On the other hand, arsenic vacancies are positively charged in *p*-type materials and so can be present in *p*-type GaAs(Zn). The formation of $V_{\text{As}} - \text{Zn}$ complex has been proposed in *p*-type GaAs(Zn).³⁸ If these complexes exist, the positron behavior implies that the arsenic vacancies are positively charged.

Our last comment is that the previous measurements done on a highly Zn-doped sample by Dlubek *et al.*¹⁶ are in agreement with our results. The results of Dannefaer and Kerr¹⁵ agree with respect to the average lifetime $\tau = 230$ ps, but the authors decompose the spectra, which we find to be of single component.

B. Bulk annihilation in semi-insulating GaAs

The positron behavior in semi-insulating GaAs materials is similar to that in *p*-type GaAs(Zn). The lifetime both for doped (In or Cr) and undoped samples is 232 ps independent of temperature. Negative or neutral vacan-

cy defects are therefore absent. One can again exclude the presence of gallium vacancies in the samples, but nothing can be concluded on the arsenic vacancies, which in these samples are positive.

The dominant defect in semi-insulating materials is *EL2*. Several models have been proposed for *EL2*. The models $\text{As}_{\text{Ga}}-\text{As}$, $\text{As}_{\text{Ga}}-\text{As}_{\text{Ga}}$, and $V_{\text{As}}-\text{As}_{\text{Ga}}$ are compatible with the behavior of positrons, since these defects in semi-insulating materials are positive. We recall that the last model is in disagreement with the EPR measurements of von Bardeleben.³⁴

Again, we remark that some previous measurements performed in polycrystals or single crystals of *si* GaAs (Refs. 13 and 16) are consistent with our results and some are not.¹⁵ As we have investigated samples provided by different laboratories and grown under different conditions, the disagreement reflects rather a discrepancy in the data analysis and interpretations than an effect of the sample preparation.

C. Annihilation in monovacancy-type defects in *n*-type GaAs

In Sec. III it has been shown that in *n*-type GaAs materials, the average positron lifetime ranges from 240 to 270 ps depending on the temperature and doping conditions. The annihilation state P1, i.e., the 295-ps lifetime, appears in *n*-type GaAs doped by Te or Sn and the annihilation state P2, i.e., the 258-ps lifetime, in *n*-type GaAs doped by Te, Sn, or Si. As mentioned in Sec. IV, positron lifetime is a parameter not very sensitive to the decoration of the vacancies. Doppler broadening of the 511-keV annihilation line could give some information on the decoration of the vacancies in doped GaAs.

A priori, we will retain the statement that the existence of native monovacancies is only slightly affected by the nature of the donor Te, Sn, or Si. In agreement with this statement, the 295-ps lifetime has been also previously found at room temperature in undoped but lightly *n*-type GaAs by Dlubek *et al.*¹⁶ and by Dannefaer *et al.*¹⁵

If we assume that the decoration of single vacancies has little effect on the position of their charge transition, the positron P1 and P2 may contain gallium vacancies or arsenic vacancies, since they are both neutral or negative in *n*-type materials (see Sec. IV C). For a further identification of the defects P1 and P2, we turn to the conditions under which the two annihilation states 295 and 258 ps exist.

VII. NATIVE VACANCY DEFECTS IN *n*-TYPE GaAs

In *n*-type GaAs materials, the existence of the 295- and 258-ps annihilation states depends on the temperature and the doping level of the materials (see Sec. III). In our analysis of the positron behavior, we will distinguish three levels of doping: light ($n \approx 10^{16} \text{ cm}^{-3}$), medium ($n \approx 10^{17} \text{ cm}^{-3}$), and heavy ($n \approx 10^{18} \text{ cm}^{-3}$). We will show that the temperature effects, the annealing effects, and the irradiation effects suggest that the 295- and 258-ps annihilation states correspond to two configurations of a same native defect.

A. Temperature effects

In the lightly Te- and Sn-doped specimens, the temperature has a surprising effect on the positron behavior: the average lifetime goes through a maximum at about 200 K and the lifetime spectra are decomposed in different ways below and above the maximum. When the doping level increases, the temperature effects become smaller and almost disappear in heavily *n*-type doped GaAs (Figs. 1–6 in Sec. III B).

1. *As-grown n-type GaAs* ($n: 10^{16} \text{ cm}^{-3}$)

The temperature effects in GaAs(Te: 1.5×10^{16}) and GaAs(Sn: 1×10^{16}) (Figs. 4 and 5) are very similar.

Between 280 and 400 K, the 295-ps lifetime component due to the vacancy defect P1 is resolved in the spectra of both samples. The positron trapping model with one type of defect is well fulfilled in this temperature region. The vacancy defect P1 is the major positron trap between 280–400 K in both samples. The trapping into the vacancy defect P1 decreases with increasing temperature: Figs. 4 and 5 show that the intensity I_2 of the lifetime 295 ps decreases and the lifetime τ_1 increases strongly with increasing temperature. At 400 K the average lifetime has reached almost the bulk level. This means that the trapping into the defect P1 disappears in a reversible way and is gradually replaced by bulk annihilation at high temperatures.

Below 280 K in GaAs(Te: 1.5×10^{16}) and below 200 K in GaAs(Sn: 1×10^{16}) the lifetime τ_2 decreases continuously with decreasing temperature from about 295 to 258 ps at 100 K. This shows that the positron trap P1 is replaced at 100 K by the positron trap P2. The one-defect trapping model ceases progressively to be valid below 280 K, and the lifetime τ_1 takes higher values than the ones calculated in the one-defect trapping model. At low temperatures the decomposition of the spectra becomes difficult, because the difference between τ_1 and τ_2 decreases. Lifetime measurements in other *n*-type GaAs samples between 20–100 K (Refs. 12 and 25) have revealed that τ_1 approaches to the bulk value of 232 ps when the temperature decreases. This increase is correlated to a strong reduction in the positron diffusion length measured using a slow positron beam.³⁹ These two facts indicate that there are additional shallow positron traps, most probably negative ions, which due to the weak binding of positrons are active only at low temperatures.³⁹ The annihilations from the shallow traps are mixed into the first lifetime component τ_1 , whereas the second lifetime τ_2 is purely due to vacancy defects.

2. *As-grown n-type GaAs* ($n: 10^{17} \text{ cm}^{-3}$)

At the medium doping level the maximum in the average lifetime is less pronounced than at the light doping level (Fig. 2). The decomposition results of GaAs(Sn: 10^{17}) (Fig. 6) are interesting. They show that τ_2 presents also a transition from values of about 258 ps to values of about 295 ps when the temperature is increased. Again at low temperatures from 80 to 250 K we find the defect P2 (258 ps), and well above room temperature at 400–500

K the decomposition seems to give partially the defects P1 (295 ps). This is the same behavior as found in lightly doped n -type GaAs in Figs. 4 and 5, but the transition of τ_2 has now shifted to higher temperatures. Between 280–400 K trapping into the defect P2 competes with trapping into the defect P1 at medium doping level when only trapping into the defect P1 is seen at light doping level.

3. As-grown n -type GaAs ($n: 10^{18} \text{ cm}^{-3}$)

The temperature effects in the heavily n -type doped samples are small. The average lifetime in Fig. 3 changes only a few ps. The defect P2 (258 ps) is found at 300 K (Table III). All the spectra measured below 300 K can be decomposed by fixing $\tau_2 = 258$ ps and no evidence of the defect P2 (295 ps) is found. The defect P2 is responsible for the positron trapping at all temperatures and dominates entirely the positron trapping at room temperature.

4. Summary

In the lightly doped n -GaAs ($n: 10^{16}$) samples the positron trapping is dominated by the defect P2 (258 ps) at low temperatures and by the defects P1 (295 ps) at high temperatures. From 100 to 200 K there is a reversible equilibrium between the trapping by P1 and P2. Above 300 K the trapping by P1 is gradually replaced by bulk annihilation.

At medium doping level of $n \approx 10^{17} \text{ cm}^{-3}$ the defect P2 is found between 80 and 250 K and the transition from P2 to P1 is shifted to above room temperature.

At high doping level of $n \approx 10^{18} \text{ cm}^{-3}$ only the defect P2 is found to trap positrons. To explain the reversible equilibrium of the trappings by P1 and P2 we will consider two models in the next section.

B. Lifetime transition 258 ps \rightarrow 295 ps and Fermi level

The reversible equilibrium between the annihilations in the monovacancy-type defects P2 (258 ps) and P1 (295 ps) may reflect two situations, one in which the defects P1 and P2 coexist at all temperatures, or the other in which P2 replaces P1 at low temperatures. We have to distinguish each of them to discuss the origin of the equilibrium $P2 \rightarrow P1$.

In the first model, P1 and P2 are two distinct monovacancy-type defects present at all temperatures. The equilibrium between the annihilation states P2 and P1 results from the different temperature dependence of the specific trapping rate in P1 and P2.

In the second model, the defects P2 and P1 are two configurations of a same monovacancy defect. There is a reversible equilibrium between these two configurations, which depends on temperature and doping level. The configuration P2 is stable at lower temperatures, whereas the configuration P1 is stable at higher temperatures.

We have to examine now, which model is consistent with the other properties of the defects P1 and P2 that we determine from the results in Sec. III. These properties, that we will discuss below, can be summarized as follows:

(i) the trapping into P1 and P2 begins to disappear in the same annealing temperature region of 700–800 K (see Secs. III and VII D); (ii) the trapping into P1 and P2 disappear after electron irradiation when the dose is sufficient to compensate the materials (see Sec. III and VII E); and (iii) the trapping into P1 is shifted to higher temperatures when doping level increases and only the trapping into P2 exists in GaAs ($n: 10^{18}$) (see Secs. III and VII A).

On the basis of the properties (i) and (ii), we eliminate the first model. We retain the second one in which a native vacancy defect gives rise to two configurations P1 and P2 in n -GaAs (10^{16}).

The property (iii) suggests that the respective existences of P1 and P2 are related to the position of the Fermi level. The reversible equilibrium between the trapping by P1 and P2 in n -type doped GaAs (10^{16} and 10^{17}) is governed by the position of the Fermi level. It appears to be temperature dependent, because the position of the Fermi level moves with temperature and crosses the energy level, where the configuration P2 transforms into the configuration P1. In Fig. 9, we have plotted the variation of the Fermi level E_F as a function of temperature in n -type GaAs at concentrations $n = 10^{16}$, 10^{17} , and 10^{18} cm^{-3} . In the calculation, only one donor level at $E_C - 3$ meV is used, and the concentrations correspond to carrier concentrations at 300 K. The lower the doping level is, the faster the Fermi level decreases below the conduction band E_C with increasing temperature. At 400 K in a sample with $n = 10^{16} \text{ cm}^{-3}$ the Fermi level drops down to $E_F = E_C - 0.15$ eV.

The transition $P2 \rightarrow P1$ (258 \rightarrow 295 ps) occurs between 100 and 210 K in Figs. 4 and 5 and between 250 and 500 K in Fig. 6, i.e., when the Fermi level drops from $E_C - 0.02$ eV to about $E_C - 0.05$ eV. In Fig. 10 we have plotted the lifetime τ_2 as a function of the Fermi-level position $E_C - E_F$ in GaAs (Te: 1.5×10^{16}), GaAs (Sn: 1×10^{16}), and GaAs (Sn: 1×10^{17}). In all these three samples the transition $P2 \rightarrow P1$ (258 \rightarrow 295 ps) occurs at the same position $E_F = E_C - 0.035 \pm 0.015$ eV. The width of the transition is in agreement with the Fermi function describing the level population, and it is wider in GaAs (Sn: 1×10^{17}) because of the higher transition tem-

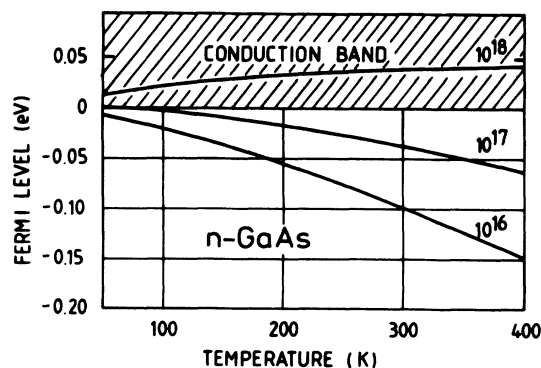


FIG. 9. Fermi-level position as a function of temperature Te-doped n -type GaAs. The concentrations given in the figure correspond to carrier concentrations at 300 K.

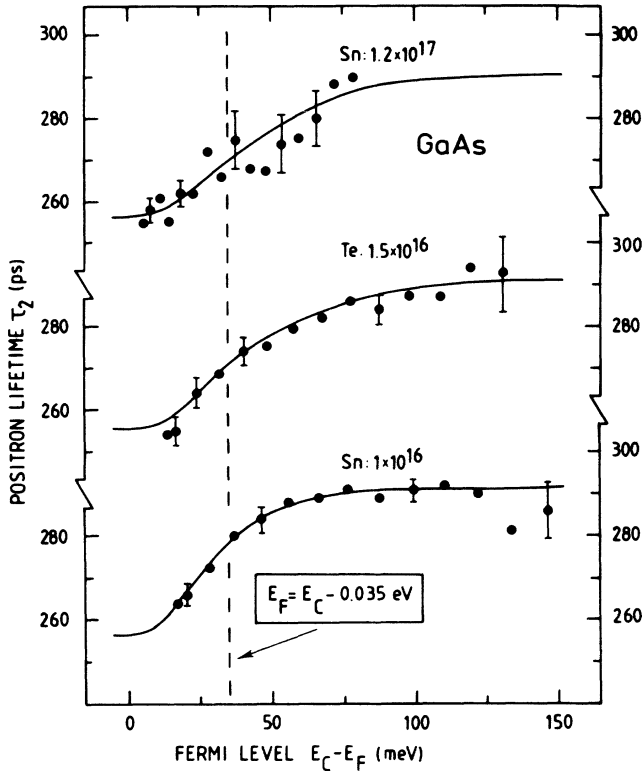


FIG. 10. Transition of the positron lifetime τ_2 at the vacancy as a function of the Fermi-level position in the energy gap. The solid lines illustrate the Fermi distribution between the two annihilation states corresponding to lifetimes $\tau_2=258$ and $\tau_2=295$ ps, respectively. The dashed line indicates the position of the vacancy ionization level at $E_C-0.035$ eV.

perature. The defect P2 (258 ps) is thus the stable configuration when the Fermi level is close to the conduction band. This is also consistent with the results of the heavily n -doped GaAs ($n: 10^{18}$) samples. As mentioned earlier (Sec. VII A 3), at any temperatures only 258-ps lifetime has been found in these samples for trapped positrons. According to Fig. 9, at $n = 10^{18} \text{ cm}^{-3}$ the Fermi level remains inside or very close to the conduction band and well above $E_C-0.035$ eV so that P2 is the stable configuration at any temperature.

C. Native monovacancies in n -type GaAs

We have arrived at the conclusion that the native vacancy involved in P2 and P1 presents two configurations in the upper half of the gap. The transition between the two configurations occurs at the Fermi-level position $E_F = E_C - 0.035$ eV. We have to examine now whether this property can be satisfied by V_{As} or V_{Ga} , the two possible identifications for a native vacancy in GaAs.

In the literature, various works indicate that the arsenic vacancy presents several charge states in the gap,^{29,33,36,37} although exceptions also exist.^{34,35} The estimated ionization levels fall in the energy range where

the Fermi level moves between 100 and 250 K in GaAs ($n: 10^{16}$). In particular, it has been proposed that a charge-state transition occurring at about or below $E_C - 0.02$ eV corresponds to $- \rightarrow 0$ (Ref. 33) and more recently, to $2- \rightarrow -$.^{35,36} So, by assuming that the native vacancy defect in n -type GaAs involves V_{As} , we can consistently explain the transition $P2 \rightarrow P1$ by the charge-state transition $2- \rightarrow -$ (or $- \rightarrow 0$). The transition $2- \rightarrow -$ (or $- \rightarrow 0$) induces a strong rearrangement of the lattice around the vacancy, since the lifetime increases from 258 to 295 ps. This rearrangement may reflect that, as expected, the Jahn-Teller distortions affecting V_{As}^- and V_{As}^{2-} have different symmetry. By comparison with the silicon vacancy, a distortion of tetragonal symmetry is expected in V_{As}^- and a mixed symmetry, tetragonal plus trigonal in V_{As}^{2-} .³⁵ The lifetime is longer in the less negative vacancy meaning that the nearest-neighbor atoms are more distant from the center possibly due to tetragonal distortion. Recent calculations³¹ show that a 5% breathing relaxation in the tetragonal mode is sufficient to increase the positron lifetime of about 30 ps.

There is common agreement^{29,33-37} that the gallium vacancy keeps the same charge state in the upper half of the gap but presents an instability of the ionic configuration. The configuration V_{Ga} is stable when the Fermi level is high in the gap and is relaxed to the configuration $V_{\text{As}} - \text{As}_{\text{Ga}}$ in semi-insulating materials.^{34,40-42} The exact position of the Fermi level for this transition is not known.^{34,40,42} The assumption that the native vacancy defect in GaAs involves V_{Ga} implies that the transition $P2 \rightarrow P1$ located at $E_C - 0.03$ eV corresponds to $V_{\text{Ga}} \rightarrow V_{\text{As}} - \text{As}_{\text{Ga}}$. This identification gives a shorter lifetime in the gallium vacancy than in the arsenic vacancy, which reproduces the trends of Puska's calculations.²⁹ It assigns to the instability of V_{Ga} an energy level which is high in the gap as it is suggested by von Bardeleben *et al.*,⁴⁰ but higher than calculated by Baraff and Schlüter.^{34,35} Here, the transition level is close to the ionization level of the charge transition of the arsenic vacancy $2- \rightarrow -$, which suggests that the instability $V_{\text{Ga}} \rightarrow V_{\text{As}} - \text{As}_{\text{Ga}}$ is induced by this charge-state transition.

Two consequences of the above identifications are worth noting. First, both cases imply that the native vacancy defects are electrically active. Second, in both of them, the defect P1 (295 ps) involves an arsenic vacancy. If the native intrinsic defects seen in lightly Te- and Sn-doped samples are also present in semi-insulating materials, one can understand why positrons do not see them: arsenic vacancies are positive in semi-insulating materials and therefore unable to trap positrons, in agreement with the absence of positron trapping found in semi-insulating and p -type materials.

At last, we have to explain why in n -GaAs ($n: 10^{16}$) the configuration P1 ceases completely to trap positrons above 350 K. The reversible transition $295 \rightarrow 233$ ps may be a Fermi controlled one. If we assume that this transition is due to a charge change of the native vacancy defect, we can calculate the position of the ionization level from the temperature variation of the positron trapping into the defects P1 (295 ps). In Fig. 11 we have plotted

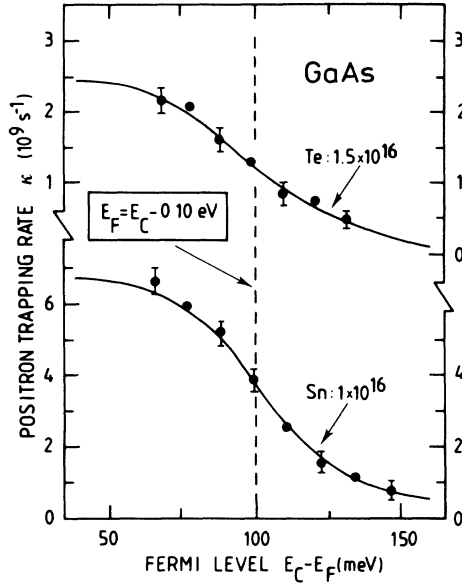


FIG. 11. Disappearance of the positron trapping as a function of the Fermi level. The solid lines illustrate the Fermi distribution between the two annihilation states corresponding to lifetimes $\tau_2 = 295$ ps (trapping to vacancies) and $\tau_b = 232$ ps (no positron trapping). The dashed line indicates the position of the vacancy ionization level at $E_C - 0.10$ eV.

the positron trapping rate as a function of the Fermi-level position in GaAs(Te: 1.5×10^{16}) and GaAs(Sn: 1×10^{16}). The trapping rates have been calculated from Eq. (8) using the results in Figs. 4 and 5 between 250 and 400 K. The widths of both transitions are again comparable to that of the Fermi function and the transition is centered at $E_F = 0.10 \pm 0.02$ eV. This value is close to the ionization level of $E_C - 0.145$ eV, where Pons and Bourgoïn³⁷ have proposed that the arsenic vacancy would undergo the charge transition $- \rightarrow 0$, and higher than that of $E_C - 0.180$ eV given by Loualiche *et al.*³⁶ The recent theoretical level for the transition $V_{As}^- \rightarrow V_{As}^0$ calculated by Puska⁴¹ using the linear-muffin-tin-orbital (LMTO) Green's-function method is 0.220 eV. By ascribing the transition $295 \rightarrow 233$ ps to the charge transition $V_{As}^- \rightarrow V_{As}^0$, we arrive at the conclusion that neutral arsenic vacancies are much less effective positron traps than the negatively charged ones.

D. Annealing of as-grown *n*-type GaAs

The annealings of GaAs(Sn: 1.6×10^{16}), GaAs(Te: 1.5×10^{16}), and GaAs(Te: 2×10^{17}) shown in Figs. 7–8 (Sec. III C) indicate that the defect P1 disappears above 700 K. This temperature range is well above the migration temperature of the arsenic interstitial, presumed to be around 500 K and of the gallium interstitial presumed to be around 4 K. Consequently, this stage is not due to the recombination of Frenkel pairs. Recent EPR measurements under photoexcitation by von Bardeleben *et al.*⁴³ have shown that a new EPR signal is generated in semi-insulating GaAs after annealing at $T \geq 720$ K. The

authors correlate the appearance of this new signal to the possible injection of mobile As interstitials in the lattice from As precipitates anchored near dislocations and dissolved by annealing at $T \geq 720$ K. If such a mechanism occurs also in lightly doped *n*-type GaAs, the recombination reaction of the interstitials with the vacancy defects explains the presence of the 700-K annealing stage observed by positron annihilation in *n*-type materials.

In lightly doped *n*-type GaAs materials, we have proposed two alternative structures for the defect P1, either V_{As} or $V_{As} - As_{Ga}$. Let us remark that the recombination of these structures with interstitials leads to different defects. The reaction $(V_{As} + As_i)$ leads to the vanishing of V_{As} vacancy defects while the reaction $(V_{As} - As_{Ga} + As_i)$ leads to the formation of As_{Ga} antisite defects. Now let us assume that the defect P1 exists also in semi-insulating material. It is then positively charged and thus not seen by positrons. If the structure of P1 involves $V_{As} - As_{Ga}$, we arrive at the conclusion that the EPR spectrum due to single antisites appear. According to Ref. 43, such signals do not appear: the EPR signals due to the As_{Ga}^x ($x = +$) arise from $As_i - As_{Ga}$ pairs before heating at 720 K and remain unchanged in semi-insulating material after heating above 720 K. This gives us an argument, although not very direct, to support the model in which the defects P1 are arsenic vacancies rather than gallium vacancies.

Measurements performed at 100 K show that the lifetime has decreased also to 231 ps after annealing at 800 K. The defect P2 has also disappeared. We have proposed for the defect P2 the structure V_{As} or V_{Ga} . Its recombination with interstitials will lead to a new defect only in the case of V_{Ga} . This new defect will be the antisite without decoration by an arsenic interstitial. Again, reasoning as above, we arrive at the conclusion that in semi-insulating materials the spectra of the antisites must change. This is, however, not observed according to Ref. 43. We therefore conclude that the defects P2 are also arsenic vacancies rather than gallium vacancies.

E. Irradiation effects in *n*-type GaAs ($n: 10^{16} \text{ cm}^{-3}$)

In Table IV, after 300-K irradiation at a dose sufficient to compensate the lightly doped samples, the lifetime at 300 K has decreased and reached values about 233 ± 1 ps. This means that the initial native vacancy defects P1 cease to trap positrons after irradiation. The same is observed for measurements done at 100 K and thus the initial vacancy defects P2 cease also to trap positrons. This means that when the trapping by the defect P1 disappears, the trapping by the defect P2 disappears. Again P1 and P2 exhibit similar properties, which supports further the conclusion that they are related to the same native vacancy defect.

We attribute the disappearance of positron trapping after irradiation to the change of the charge state of the defects due to compensation and this will be discussed elsewhere.²³ The positron traps become positive involving V_{As}^+ .

F. Concentrations of the defects P1 and P2

In the framework of the trapping model, we can calculate the total trapping rates into the defects P1 or P2 from Eq. (6) (Sec. VI C). In Secs. VII A–C we have seen that P1 and P2 are negatively charged, their charge being $-$ for P1 and $2-$ for P2. In order to calculate the concentration of native monovacancies giving rise to P1 and P2, we take a specific trapping rate per defect P1 and P2 equal to $6 \times 10^{-9} \text{ s}^{-1} \text{ cm}^{-3}$.²² The concentration of native monovacancies obtained in this way and given in Table V is overestimated, since it has been seen in Sec. IV B that the specific trapping rate is probably higher in negatively charged defects. In addition, the specific trapping rate into the defect P2 is probably higher than that into the defect P1, since the defect P2 is more negative than the defect P1.

To obtain the concentrations of native vacancy defects, we have to correct by a factor of about 2 the concentrations of defects P1 to compensate their disappearance in the transition 295 \rightarrow 232 ps taking place at 300 K in lightly n -type doped samples (Sec. VII A 2). Such a correction is not necessary for the defects P2 because at 300 K in the heavily n -type doped samples, the Fermi level is still in the conduction band and so far from the transition P2 \rightarrow P1. We found the concentrations of native monovacancies of the order of 10^{17} cm^{-3} . Such concentrations are of the order of the values determined by x-ray diffraction for the nonstoichiometric defects⁴⁴ but they are higher than the defect concentrations of $5 \times 10^{16} \text{ cm}^{-3}$ measured by deep-level transient spectroscopy (DLTS) for electron trap defects. In our model, the native monovacancies are electrically active but apparently not directly detected by DLTS. This is consistent with the results of Bol'Cheva *et al.*,⁴⁵ who studied by DLTS the evolution of the electron traps as a function of the concentration and nature of the donors. They concluded that intrinsic native defects must exist in high concentrations ($10^{18} - 10^{19} \text{ cm}^{-3}$) in order to explain their results.

A question to elucidate is, why techniques like the deep-level transient spectroscopy (DLTS) and the deep-level optical spectroscopy (DLOS) do not detect in as-grown n -type GaAs the vacancy defects which are found in electron irradiated samples.^{36,37} From the point of view of positrons, the defects in as-grown n -type GaAs give rise to lifetimes quite similar to the vacancy defects introduced by electron irradiation.^{20–22} A reason may be that DLTS and DLOS are more sensitive to the differences in the decoration of the vacancies than posi-

TABLE V. Total trapping rates κ at 300 K and concentrations c of the defects P1 and P2 in Te-doped GaAs samples when one type of defect (P1 or P2) is trapping positrons. The bulk lifetime is taken equal to 232 ps and a specific trapping rate of $6 \times 10^{-9} \text{ s}^{-1} \text{ cm}^{-3}$ is used.

Sample	Trap	κ (s^{-1})	c (cm^{-3})
GaAs(Te: 1.5×10^{16})	P1, 295 ps	1.3×10^9	2×10^{17}
GaAs(Te: 5.0×10^{18})	P2, 258 ps	1.1×10^9	2×10^{17}

tron lifetime data. Positron lifetime reflects the open volume of a defect and is thus rather insensitive to its surrounding.

Several models involving vacancies have been proposed for the major deep level $EL2$ in GaAs.^{1,2,46} In particular, Wager and Van Vechten⁴⁷ have proposed a model for $EL2$ based on the positron-lifetime data of Dannefaer *et al.*¹⁵ in which $EL2$ is a divacancy-arsenic-antisite defect giving rise to the 295-ps lifetime that we have also detected in n -type GaAs. However, we believe that there is no strong experimental support to attribute the 295 ps to a divacancy $V_{\text{As}} - V_{\text{Ga}}$ rather than to a monovacancy. Moreover, the analysis of our positron data shows that a model, which attributes the 295-ps lifetime to $EL2$, implies new properties of $EL2$. First, $EL2$ presents a configuration change, which takes place without photoexcitation and which is controlled by the position of the Fermi level. Second, it is from the 258-ps configuration presenting the highest electronic density in the vacancy, from which the photoexcitation in a metastable configuration is observed. Third, the 258-ps configuration must involve, in addition to a vacancy, the arsenic antisite which is believed to be a major component of the structure of $EL2$.^{1,2} Fourth, since the 258-ps configuration is the stable one when the Fermi level is high in the gap, the disappearance of As_{Ga} antisites reported by Lagowski *et al.*⁴² when the donor concentration increases must be due to a donor effect rather than to a Fermi-level effect on the stability of $EL2$.

VIII. CONCLUSION

In this paper, information on the native vacancy defects in gallium arsenide has been extracted from a systematic study of the positron-lifetime spectra in various types of GaAs materials. It has been shown that a coherent picture of the positron response emerges when its annihilation characteristics are correlated to the position of the Fermi level.

Positrons give a direct evidence of the existence of neutral or negative native vacancy defects in n -type materials. In p -type and semi-insulating GaAs, positrons do not detect native vacancy defects. Two explanations are possible: the concentration of the native vacancy defect is lower than 10^{15} cm^{-3} or their charge is positive.

In n -type materials, two types of monovacancy defects are detected. The monovacancies are isolated or associated to donors or to intrinsic point defects. Their properties are shown to fit well a model in which their stability is governed by the position of the Fermi level. It is proposed that the transition between the two defects corresponds to the charge transition of the arsenic vacancy $V_{\text{As}}^{2-} \rightarrow V_{\text{As}}^{-}$.

The stable configuration when the Fermi level is high in the gap above $E_C - 0.035 \text{ eV}$, gives rise to a lifetime of $258 \pm 3 \text{ ps}$. It is proposed to involve an arsenic vacancy V_{As}^{2-} . When the Fermi level goes below $E_C - 0.035 \text{ eV}$, this configuration is transformed to a new one involving V_{As}^{-} and giving rise to a lifetime of $295 \pm 3 \text{ ps}$. The increase of the trapped positron lifetime indicates that the charge transition $V_{\text{As}}^{2-} \rightarrow V_{\text{As}}^{-}$ induces an outwards relaxa-

tion of the lattice around the vacancy. The V_{As}^- configuration ceases to trap positrons when the Fermi level moves below $E_C - 0.10$ eV. This is suggested to correspond to the transition $V_{As}^- \rightarrow V_{As}^0$. Both V_{As}^{2-} and V_{As}^- configurations disappear after annealings about 750 K. They disappear also after electron irradiation at 300 K when the samples are compensated. We have also discussed the transition 258 \rightarrow 295 ps in a model based on the two configurations of the gallium vacancy, $V_{Ga} \rightarrow V_{As} - As_{Ga}$, which we, however, consider less likely.

Within a simple scheme, in which the same native monovacancy-type defect V_{As} exists in p -type, semi-insulating, and n -type materials, we are able to explain all aspects of the positron trapping behavior. The charge

state of V_{As} changes as a function of the Fermi-level position. It is positive in p -type and semi-insulating GaAs, but neutral, single, or double negative in n -type GaAs. However, positron lifetimes do not indicate, whether V_{As} is isolated or bound to another defect or impurity.

ACKNOWLEDGMENTS

The authors are indebted to J. von Bardeleben and J. Bourgoin for discussions and critical comments. They are grateful also to B. Geoffroy and F. Pierre for their assistance in experiments.

- ¹Gallium Arsenide and Related Compounds, Proceedings of the 12th International Symposium on Gallium Arsenide and Related Compounds, edited by M. Fujimoto, IOP Conf. Serv. No. 79 (IOP, Bristol, 1985); *Deep Centers in Semiconductors: A State of the Art Approach*, edited by S. T. Pantelides (Gordon and Breach, New York, 1986).
- ²T. A. Kennedy, in *Defects in Semiconductors*, edited by H. J. von Bardeleben, Materials Science Forum (Trans Tech Publications, Switzerland, 1986), Vols. 10–12, p. 283.
- ³*Positrons in Solids*, Vol. 12 of *Topics in Current Physics*, edited by P. Hautojärvi (Springer, Heidelberg, 1979).
- ⁴*Positron Solid State Physics*, edited by W. Brandt and A. Dupasquier (North-Holland, Amsterdam, 1983).
- ⁵*Positron Annihilation*, edited by P. C. Jain, R. M. Singru, and K. P. Gopinathan (World Scientific, Singapore, 1985).
- ⁶W. Fuhs, V. Holzhauser, S. Mantl, F. W. Richter, and R. Sturm, *Phys. Status Solidi B* **89**, 69 (1978).
- ⁷S. Dannefaer, G. W. Dean, D. P. Kerr, B. G. Kerr, and B. G. Hogg, *Phys. Rev. B* **14**, 2709 (1976).
- ⁸S. Dannefaer, S. Kupca, B. G. Hogg, and D. P. Kerr, *Phys. Rev. B* **22**, 6136 (1980).
- ⁹M. Shimotomai, Y. Ohgino, H. Fukushima, Y. Nagayasu, T. Mihara, K. Inoue, and M. Doyama, in *Defects and Radiation Damage in Semiconductors, Osio, Japan, 1980*, edited by R. R. Hasiguti (IOP, Bristol, 1981), Vol. 49, p. 241.
- ¹⁰S. Dannefaer, N. Fruensgaard, S. Kupca, B. G. Hogg, and D. Kerr, *Can. J. Phys.* **61**, 451 (1983).
- ¹¹J. L. Cheung, J. P. Karins, J. V. Corbett, and L. C. Kimerling, *J. Appl. Phys.* **50**, 2962 (1979).
- ¹²D. P. Kerr, S. Kupca, and B. G. Hogg, *Phys. Lett.* **88A**, 429 (1982).
- ¹³S. Dannefaer, *J. Phys. C* **15**, 599 (1982).
- ¹⁴S. Dannefaer, D. P. Kerr, and B. G. Hogg, *Phys. Rev. B* **30**, 3355 (1984).
- ¹⁵S. Dannefaer and D. P. Kerr, *J. Appl. Phys.* **60**, 591 (1986).
- ¹⁶G. Dlubek, O. Brümmer, F. Plazaola, and P. Hautojärvi, *J. Phys. C* **19**, 3318 (1986).
- ¹⁷G. Dlubek, O. Brümmer, F. Plazaola, P. Hautojärvi, and K. Naukkarinen, *Appl. Phys. Lett.* **46**, 1136 (1985).
- ¹⁸S. Dannefaer, *Phys. Status Solidi A* **102**, 481 (1987).
- ¹⁹G. Dlubek and R. Krause, *Phys. Status Solidi A* **102**, 443 (1987).
- ²⁰M. Stucky, R. Paulin, B. Geoffroy, C. Corbel, and J. Suski, in *Positron Annihilation*, Ref. 5, p. 714.
- ²¹C. Corbel, P. Moser, and M. Stucky, *Ann. Chim. (Paris)* **8**, 733 (1985).
- ²²M. Stucky, C. Corbel, B. Geoffroy, P. Moser, and P. Hautojärvi, in *Defects in Semiconductors*, Ref. 2, p. 265.
- ²³M. Stucky, Ph.D. thesis, Commissariat à l'Énergie Atomique, Rapport CEA (1987); C. Corbel, M. Stucky, P. Hautojärvi, and P. Moser (unpublished).
- ²⁴P. Hautojärvi, P. Moser, M. Stucky, C. Corbel, and F. Plazaola, *Appl. Phys. Lett.* **48**, 809 (1986).
- ²⁵K. Saarinen, Masters thesis, Helsinki University of Technology, 1987.
- ²⁶A. Vehanen, P. Hautojärvi, J. Johansson, J. Yli-Kaupilla, and P. Moser, *Phys. Rev. B* **25**, 762 (1982).
- ²⁷Y. K. Part, J. T. Waber, M. Meshii, and C. L. Snead, Jr., *Phys. Rev. B* **34**, 823 (1986).
- ²⁸W. Brandt, *Appl. Phys.* **5**, 1 (1984); R. N. West, in *Positron Solid State Physics*, Ref. 3, p. 89.
- ²⁹M. J. Puska, O. Jepsen, O. Gunnarsson, and R. M. Nieminen, *Phys. Rev. B* **34**, 2965 (1986); M. J. Puska, in *Defects in Semiconductors*, Ref. 2, p. 277; M. J. Puska, *Phys. Status Solidi A* **102**, 11 (1987).
- ³⁰C. Corbel, Commissariat à l'Énergie Atomique, Rapport CEA-R-5334 (1986); C. Corbel, M. Puska, and R. M. Nieminen, *Rad. Eff.* **79**, 305 (1983).
- ³¹M. Puska and C. Corbel, *Phys. Rev. B* (to be published).
- ³²M. Puska and R. M. Nieminen, *J. Phys. F* **13**, 333 (1983).
- ³³J. van der Rest and P. Pecheur, *J. Phys. C* **17**, 85 (1984).
- ³⁴G. A. Baraff and M. Schlüter, *Phys. Rev. Lett.* **55**, 2340 (1985).
- ³⁵G. A. Baraff, in *Defects in Semiconductors*, Ref. 2, p. 293.
- ³⁶S. Loualiche, A. Nouailhat, G. Guillot, and M. Lannoo, *Phys. Rev. B* **20**, 5822 (1984).
- ³⁷D. Pons and J. Bourgoin, *J. Phys. C* **18**, 3839 (1985).
- ³⁸C. J. Hwang, *Appl. Phys.* **39**, 4307 (1968).
- ³⁹K. Saarinen, P. Hautojärvi, A. Vehanen, R. Krause, and G. Dlubek (unpublished).
- ⁴⁰H. J. von Bardeleben, A. Miret, and J. C. Bourgoin, in *Defects in Semiconductors*, Ref. 2, p. 299.
- ⁴¹M. J. Puska (unpublished); see also *Phys. Status Solidi A* **102**, 11 (1987).
- ⁴²J. Lagowski, H. C. Gatos, J. M. Parsey, K. Wade, M. Kaminska, and W. Walukiewicz, *Appl. Phys. Lett.* **40**, 342 (1982); H. C. Gatos, J. Lagowski, J. M. Parsey, K. Wade, M. Kaminska, and W. Walukiewicz, in *Gallium Arsenide and Related Com-*

- pounds*, edited by G. E. Stillman (IOP, Bristol, 1982), Vol. 65, p. 222.
- ⁴³H. J. von Bardeleben and J. C. Bourgoin, in Proceedings of the Fourth Conference on Semi-insulating III-V Compounds, Hakone, Japan, 1986 (unpublished).
- ⁴⁴I. Fujimoto, *Jap. J. Appl. Phys.* **13**, L287 (1984).
- ⁴⁵Y. u. N. Bol'Cheva, V. V. Voronkov, R. I. Glorizova, and L.I. Kolesnik, *Fiz. Tekh. Poluprovodn.* **19**, 292 (1985) [*Sov. Phys.—Semicond.* **19**, 179 (1985)].
- ⁴⁶H. J. von Bardeleben and J. C. Bourgoin, *Phys. Rev. B* **33**, 2890 (1986).
- ⁴⁷J. F. Wager and J. A. van Vechten, *Phys. Rev. B* **35**, 2330 (1987).